# A Ring-Vortex Downburst Model for Flight Simulations

Michael Ivan*
*Boeing Computer Services Company, Seattle, Washington*

**A mathematical model of a downburst for real-time flight simulations of takeoffs and landings in low-altitude severe wind shears due to downbursts or microbursts was developed. The downburst mature stage was idealized to resemble the circulatory wind-flow patterns noted in meteorological downburst data from the Joint Airport Weather Studies (JAWS) Project. The idealization produced a three-dimensional axisymmetric circulatory flowfield similar to that around a horizontal smoke ring or ring vortex at an appropriate height above the ground. The flowfield around a ring vortex has a stream function expressed in Sir Horace Lamb's classical textbook *Hydrodynamics* in terms of the complete elliptic integrals combination of $[F(k)-E(k)]$; which is approximated herein by the expression: $[0.788k^2/(0.25+0.75\sqrt{1-k^2})]$, in the limited range of $0\le k^2\le 1$ for the modulus $k=(r_2-r_1)/(r_2-r_1)$, where $r_1$ and $r_2$ denote the least and greatest distances, respectively, of the point P from the ring vortex. "Digital differentiations" of the downburst stream function at the airplane center of gravity yield both the WZ downdraft and the WR radial wind velocity component. The latter is then resolved into the two horizontal components WX and WY for wind speeds along and across the runway, respectively. Occupying 383 words of memory and having an average real-time execution time of 1.3 ms on a Harris H800 digital computer, the present ring-vortex downburst model provides economical simulation of severe wind-shear flow patterns that closely resemble some of the flow patterns noted in meteorological data from the JAWS Project.**



## Nomenclature

ACMPE = approximated complete elliptic integrals
ACMPEM = ACMPE for mirror-image ring vortex, Eq. (13)
ACMPEP = ACMPE for primary ring vortex, Eq. (11)
CG = center-of-gravity position on airplane
CIRCRV = circulation strength of primary ring vortex, Eq. (1)
Db = downburst
GSX = $X$ coordinate along runway from threshold, ft
GSY = $Y$ coordinate from runway centerline, ft
H = barometric altitude of airplane CG, ft
HGCG = center-of-gravity altitude above ground, ft
HGROUN = altitude of ground level below CG, ft
HGVORT = height above ground to primary ring vortex, ft
KMOD = $k$-modulus argument for elliptic integrals
KMODMV = KMOD for mirror-image ring vortex, Eq. (12)
KMODPV = KMOD for primary ring vortex, Eq. (10)
PSIRW = orientation angle of runway from north, deg
RCOHGV = ratio of core radius to reference height of HGVORT
RDCORE = radius of core of rotating vortex material
RDVORT = reference radius of ring vortex, ft
R-V = ring vortex
RVAXCG = radius to CG from vertical axis of downburst, Eq. (5)
R/W = runway
R1MSML = small distance "R1" from CG to mirror-image ring vortex, Eq. (7)
R1PSML = small distance "R1" from CG to primary ring vortex, Eq. (6)
R2MLRG = large distance "R2" from CG to mirror-image ring vortex, Eq. (9)
R2PLRG = large distance "R2" from CG to primary ring vortex, Eq. (8)
STRFCG = stream function at CG from ring-vortex downburst, Eq. (18)
STRFCR = stream function at unit radial increment from CG, Eq. (19)
STRFCZ = stream function at unit "$Z$" increment from CG, Eq. (17)
STRMFN = stream function at CG from ring-vortex downburst, Eq. (14)
SX,SY = CG displacement north and east respectively, from threshold of runway
WR = radial wind speed of outflow from axis, Eq. (15)
WX = horizontal tail-wind component in $X$-runway direction, Eq. (20)
WY = horizontal cross-wind component, $Y$-runway direction, Eq. (21)
WZ = downdraft wind component down "$Z$" direction, Eqs. (2) and (16)
WZREF = reference axial downdraft at height of HGVORT
XCGDBC = $X$-runway distance of CG from downburst center, Eq. (3)
XRWDBC = $X$-runway coordinate to downburst central axis
YCGDBC = $Y$-runway distance of CG from downburst center, Eq. (4)
YRWDBC = $Y$-runway coordinate to downburst central axis

Received May 19, 1985; presented as Paper 85-1749 at the AIAA Flight Simulation Technologies Conference, St. Louis, MO, July 22-24, 1985; revision received July 24, 1985. 

*Senior Engineer, Simulation Applications Software. Member AIAA.

## Introduction

A VARIETY of weather features such as mountain lee waves, thunderstorms, frontal shears, and downbursts have been tabulated in Ref. 1 as probable causes of 27 hazardous encounters with low-altitude severe wind shears. However, attention will be focused herein on the downburst wind-shear phenomenon only because this single weather feature was the probable cause of approximately half of those hazardous encounters. Usually associated with a thunderstorm, "downburst" and "microburst" are used here inter-

changeably to denote a low-altitude severe wind-shear flow pattern defined in Ref. 2 as "a downdraft-induced, diverging, horizontal flow near the surface, whose initial horizontal dimension is less than 4 kilometers, and whose differential velocity is greater than 10 meters per second."

The distinctive label of "microbursts" had been given to downbursts with wind shears greater than 10 m/s across diameters ranging from 1 to 4 km in Refs. 3 and 4, where meteorological analyses indicated a greatest probability of severe wind shears from mature downbursts with particularly critical diameters of approximately 3 km or the length of a 10,000-ft runway, as shown below the Fig. 1 wind-flow diagram. This mature outburst stage occurs after a downdraft has impinged against the ground and has been deflected initially into a horizontal radial outburst flow that later curls up from the ground to form the mature downburst flow pattern shown in Fig. 1. Circulatory wind-flow patterns similar to those around a horizontal "smoke ring" or ring vortex at an appropriate height above the ground had been noted in downburst wind-shear data from the Joint Airport Weather Studies (JAWS) Project in Refs. 2 and 5. Such microbursts can form rapidly to full intensity in less than 5 min and usually have a short duration of less than 10 min at full intensity.

Real-time flight simulations were being used to study possible solutions to the problems of airplane flights through severe wind shears. These simulations required a downburst mathematical model that would be both economical with computer resources and versatile enough to simulate a range of important parameters such as size, shape, and intensity of the downburst model. Only the low-altitude wind-flow regions within, say, 500 ft of the ground are of primary concern for physically realistic simulations of severe wind shears because these low-altitude winds will have the most critical effects on the flight-path trajectory of an airplane relative to the ground. An initial candidate for a fairly realistic simulation of the preceding mature downburst model was a three-dimensional axisymmetric flowfield developed in Ref. 6 between two circular horizontal doublet sheets with suitable radial distributions of the singularity intensity. The primary doublet sheet above ground level was matched below ground level by a mirror-image second doublet sheet with opposite sign to satisfy the boundary condition for only horizontal flow velocity along the ground level.

In Ref. 6 the major attention was focused on a downburst model based on a cosine radial distribution of the doublet singularity intensity, and that cosine distribution required extensive integrations to calculate the resulting flowfield. However, some flow data also shown in Ref. 6 were for a simple downburst model based on a uniform distribution of the doublet-sheet singularity. It was noted that the flowfield from such a uniform doublet distribution corresponded also to that from two ring vortices in place of the two circular edges of the doublet sheets. Thus, the present downburst model is based on the simple concept of two ring vortices producing a flowfield that could be calculated easily in a "closed-form solution" not requiring extensive integrations.

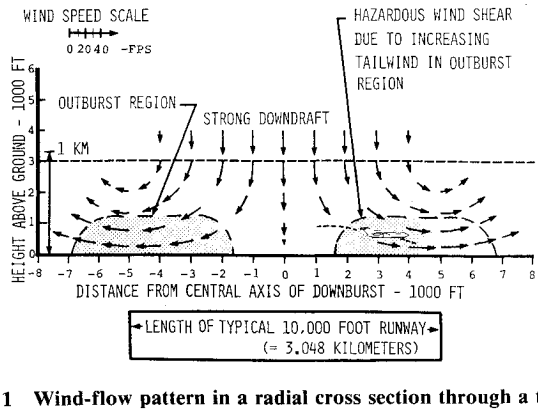


**Fig. 1 Wind-flow pattern in a radial cross section through a typical microburst as a hazardous, mature downburst.**

## Stream Function for Ring-Vortex Downburst

The simplicity of the latter downburst model based on two ring vortices was enhanced by the use of the classical "closed-form" equations [see Ref. 7, p. 237, Eqs. (11) and (12)] for the stream function for the flowfield around an isolated ring vortex. A constant value of the stream function will define the coordinates along a steady streamline in that flowfield even though the streamline pattern in a downburst may be of academic interest only. However, the downburst's velocity components are of prime importance for flight simulations and will be calculated later from the stream function by appropriate differentiations [per Ref. 7, p. 236, Eq. (1)] to yield the radial and axial velocity components.

The ring-vortex stream function in Eq. (11) of Ref. 7 is expressed in terms of the following combination of the complete elliptic integrals: $[F(k)\text{-}E(k)]$. These "higher functions" are described in Ref. 8, pp. 43-61. The present model calculates the downburst stream function at a point P by approximating the combination $[F(k)\text{-}E(k)]$ with the expression $[(0.788k^2)/(0.25+0.75\sqrt{1-k^2})]$ in the limited range of $0 \le k^2 \le 1$ for the modulus $k=(r_2-r_1)/(r_2+r_1)$, where $r_1$ and $r_2$ denote the least and greatest distances, respectively, of point P from the ring vortex.

Figure 2 represents an oblique overview of a ring-vortex downburst model positioned in runway-oriented coordinates to the right of the takeoff end of a runway. Figure 3 presents an enlarged oblique view of the ring-vortex downburst model to show some of the geometric details that enter into the calculations of first the stream function, STRMFN, and then the runway-oriented wind-shear velocity components WX, WY, and WZ.

Default data values will be enclosed in parentheses to indicate appropriate typical values and units for some of the input parameters used to define a downburst model classified as producing medium-intensity wind shears. The downburst model shown in Figs. 2 and 3 is based on a horizontal ring vortex with a reference radius RDVORT (=5000 ft) located above ground level at a reference height of HGVORT (=3000 ft), at which altitude a reference downdraft velocity of WZREF (=35 ft/s) will flow down the central axis. Either doubling or halving the WZREF reference downdraft velocity will proportionately either increase the wind shears to a high-intensity category or decrease the wind shears to a low-intensity category, respectively.

The velocities in this downburst model are proportional to the circulation strength of the primary ring vortex, CIRCRV, which is related to the WZREF reference downdraft through the following equation:

$$\text{CIRCRV} = \frac{\text{WZREF} * (2 * \text{RDVORT})}{\left\{ \underbrace{1}_{\text{Primary ring-vortex effect}} \quad \underbrace{\frac{-1}{\left[1+\left(\frac{2*\text{HGVORT}}{\text{RDVORT}}\right)^2\right]^{1.5}}}_{\text{Mirror-image effect}} \right\}} \tag{1}$$

Equation (1) shows both the effect of the "imaginary mirror-image ring vortex," assumed to be below ground level, and the effect of the "primary ring vortex" above ground level. The above equation is based on an equation presented in Ref. 9, p. 93, in relation to Fig. 2.13.5 shown there for "velocity induced by a circular vortex ring at a point on the axis." This latter equation was also used to develop the following equation (2) for the WZ downdraft velocity down the vertical central axis

of the downburst model:

$$WZ = \left(\frac{CIRCRV}{2*RDVORT}\right)*\left\{\underbrace{\frac{1}{\left[1+\left(\frac{HGVORT-HGCG}{RDVORT}\right)^2\right]^{1.5}}}_{\text{Primary ring-vortex effect}} - \underbrace{\frac{1}{\left[1+\left(\frac{-HGVORT-GCG}{RDVORT}\right)^2\right]^{1.5}}}_{\text{Mirror-image effect}}\right\}$$

As expected, the downdraft velocity in eq. (2) diminishes to zero at the stagnation point at ground level where HGCG = 0.

The ring-vortex downburst model has radial symmetry about its vertical central axis; and Shown in Fig. 2 is the radial distance, RVAXCG, calculated as follows from that vertical axis to the CG of the airplane:

$$XCGDBC = GSX - XRWDBC \quad (3)$$

$$YCGDBC = GSY - YRWDBC \quad (4)$$

$$RVAXCG = \sqrt{(XCGDBC(^2 + (YCGDBC)^2} \quad (5)$$

In the radial plane that contains RVAXCG, there are also the following four important distances measured from the CG as shown in Fig. 3:

R1PSML and R1MSML as the small (least) distances "R1" from CG to, respectively, the "primary" and "mirror-image" ring vortices:

R1PSML

$$= \sqrt{(HGCG - HGVORT)^2 + (RVAXCG - RDVORT)^2} \quad (6)$$

R1MSML

$$= \sqrt{(HGCG + HGVORT)^2 + (RVAXCG - RDVORT)^2} \quad (7)$$

R2PLRG and R2MLRG as the large (greatest) distances "R2" from CG to, respectively, the "primary" and "mirror-image" ring vortices:

R2PLRG

$$= \sqrt{(HGCG - HGVORT)^2 + (RVAXCG + RDVORT)^2} \quad (8)$$

R2MLRG

$$= \sqrt{(HGCG + HGVORT)^2 + (RVAXCG + RDVORT)^2} \quad (9)$$

The preceding "R1" and "R2" distances to the "primary" ring vortex were used to calculate the KMODPV as the corresponding "*k*-modulus" argument for the following ACMPEP "approximation for the complete elliptic integrals applicable to the primary ring vortex":

KMODPV

$$= (R2PLRG - R1PSML)/(R2PLRG + R1PSML) \quad (10)$$

ACMPEP

$$= (0.788*KMODPV^2)/(0.25 + 0.75\sqrt{1 - KMODPV^2}) \quad (11)$$

Similarly, the following corresponding KMODMV and ACMPEM were calculated for the "mirror-image ring vortex":

KMODMV

$$= (R2MLRG - R1MSML)/(R2MLRG + R1MSML) \quad (12)$$

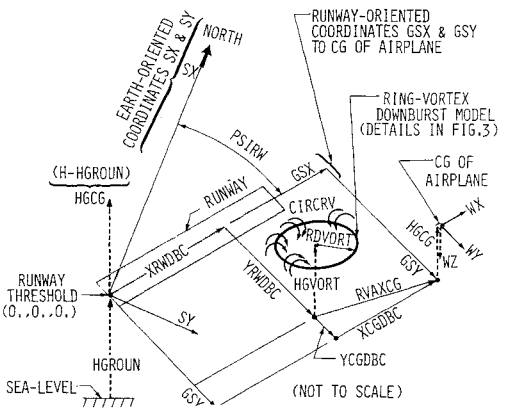


**Fig. 2 Oblique overview of ring-vortex downbursst model.**

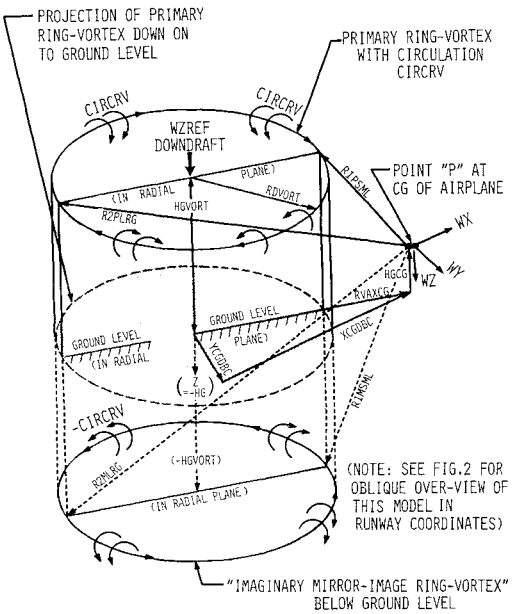


**Fig. 3 Geometric details of ring-vortex downburst model.**

ACMPEM

$$= (0.788*KMODMV^2)/(0.25 + 0.75\sqrt{1 - KMODMV^2}) \quad (13)$$

Finally, the STRMFN stream function at the CG of the airplane is

STRMFN

$$= \left(\frac{-CIRCRV}{2\pi}\right)*\begin{bmatrix}(R1PSML + R2PLRG)*ACMPEP \\ -(R1MSML + R2MLRG)*ACMPEM\end{bmatrix} \quad (14)$$

## The Velocity Components of Wind Shear

On the basis of Eq. (1) of Ref. 7, p. 236, the WR radial velocity component and the WZ downdraft velocity component are related to the following mathematical derivatives and approximate "digital differentiations" of the preceding STRMFN steam function outside of the unit radius of RVAXCG:

$$WR = \frac{1}{RVAXCG}*\left[\frac{\partial(STRMFN)}{\partial(Z)}\right] \simeq \frac{(STRFCZ - STRFCG)}{RVAXCG} \quad (15)$$

$$WZ = \frac{-1}{RVAXCG} * \left[\frac{\partial(STRMFN)}{\partial(RVAXCG)}\right] \simeq \frac{(STRFCG - STRFCR)}{RVAXCG} \quad (16)$$

where

$$STRFCZ = STRMFN\,[(HGCG - 1), RVAXCG] \quad (17)$$

with a unit "$Z$" displacement applied as a unit decrement to HGCG to yield (HGCG − 1) as the revised argument for STRMFN [eq. (14)].

$$STRFCG = STRMFN(HGCG, RVAXCG)$$

at the airplane's CG (18)

$$STRFCR = STRMFN\,[HGCG, (RVAXCG + 1)] \quad (19)$$

with a unit "radial" displacement applied as a unit increment to RVAXCG

Still outside of the unit radius of RVAXCG, the preceding WR radial component is projected [using results from Eqs. (3-5)] into the following two horizontal components WX and WY in runway-oriented coordinates:

$$WX = WR * XCGDBC/RVAXCG \quad (20)$$

$$WY = WR * YCGDBC/RVAXCG \quad (21)$$

The preceding Eqs. (6-21) were arbitrarily restricted to apply outside of the unit radius of RVAXCG to avoid possible attempted division by zero as RVAXCG approached zero at the vertical central axis of this downburst model.

However, within the unit radius of RVAXCG, there is arbitrary setting to zero of the WR radial components and also both horizontal components WX and WY. In this unit radius cylindrical region, only the remaining WZ downdraft component is calculated to be the "simple" central axial downdraft based on the preceding Eq. (2).

The label of "#1 Region Central Downdraft" is applied in Fig. 4a to the unit radius cylindrical region around the central vertical axis. Also shown in Fig. 4a are the other two regions labeled as:

"#3 Region Core" – an assumed circular toroid of "core-vortex material" executing rotational flow similar to rigid-body rotation.

"#Region Irrotational Flow" – the induced irrotational flow region remaining outside of both of the preceding regions 1 and 3.

The concept behind the rigid-body rotations inside core region 3 is to calculate physically realistic velocity components through a fairly simple interpolation scheme in order to avoid the theoretically large velocities calculated near a concentrated vortex. Beginning from an arbitrary zero velocity at the center of each circular cross section of this "core," the WR and WZ velocity components are increased linearly as indicated in Fig. 4b to match the velocity components calculated on the "core" surface at a cross-sectional "core radius," RDCORE. The RDCORE is assumed to be proportional to the reference height, HGVORT, through the ratio RCOHGV, equal to 0.8 in default data.

## Sample Flow Patterns from the Downburst Model

The sample idealized downburst model shown in Fig. 4b is based on wind-shear velocity components WX and WZ calculated by a digital computer program using the noted default data values to define the size and intensity of the wind-shear model. Those data values had been selected to simulate a medium-intensity wind-shear level with a change in horizontal wind speed of 82 ft/s (= 25 m/s) occurring across a downburst model 10,000 ft in diameter. Downbursts with diameters in the general size of 10,000 ft or 3 km were indicated in Refs. 1-4 to be the critical sizes that may be hazardous to transport airplanes during takeoffs and landings.

The digital computer program for this downburst model was written in the FORTRAN 77 programming language and occupied 383 words of memory in a Harris H800 digital computer. In real-time flight simulations on that computer, this downburst model had an average execution time of 1.3 ms.

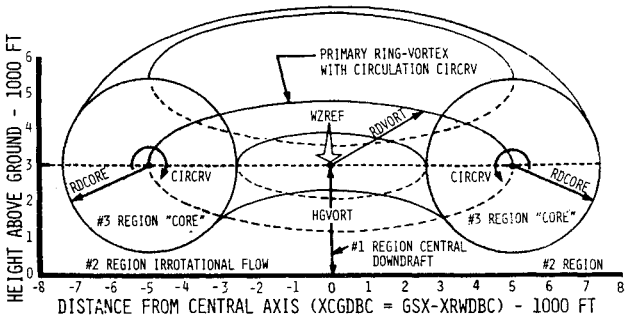


**Fig. 4a Three wind shear regions in the IVAN ring-vortex downburst model.**

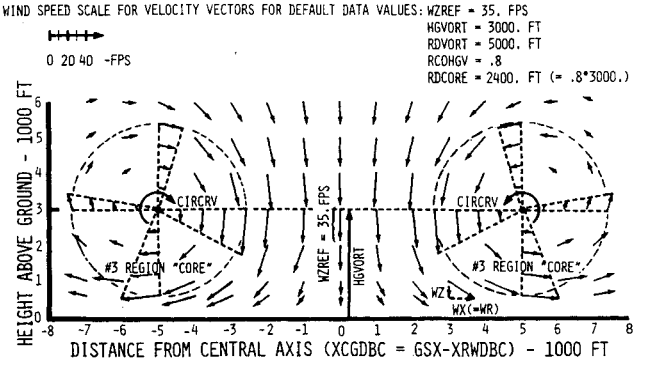


**Fig. 4b Typical wind-shear velocity vectors in a radial cross section through the downburst model.**

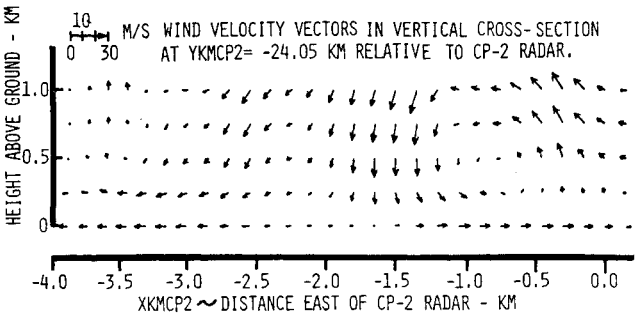


**Fig. 5a JAWS 5 August 1982 wind-shear data showing a downburst flow pattern.**

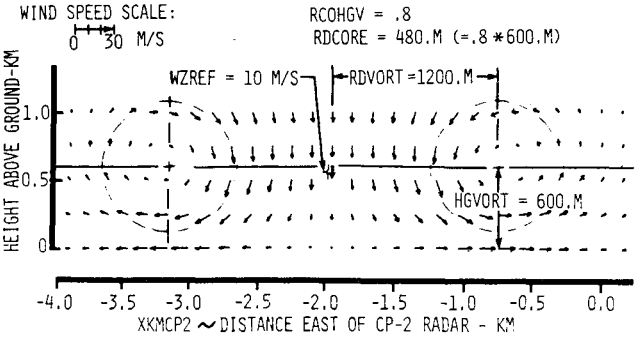


**Fig. 5b Idealized downburst model approximation of Fig. 5a JAWS data.**

Figure 5a shows a downburst flow pattern in a vertical cross section of wind components obtained from Joint Airport Weather Studies (JAWS), August 5, 1982, wind-shear data,[5] and a similar flow pattern was also shown in the July 14, 1982 JAWS wind-shear presented in Ref. 2, Fig. 2(b). Figure 5b shows calculated wind-shear velocities from the present downburst model with the noted input parameters to approximate the downburst flow pattern in Fig. 5a. Comparison of Fig. 5b with Fig. 5a indicates that the present downburst model can simulate wind-flow patterns that are physically realistic approximations of some of the major wind-flow patterns obtained from JAWS 5 August 1982 wind-shear data.

This downburst model has been implemented and used successfully in the Engineering Simulation Center at Boeing.

## Conclusions

Three features of the present version of a ring-vortex model downburst make it suitable for use in real-time simulations of airplane flights through downbursts near the ground:

1) Physically realistic approximations of some JAWS wind-vector patterns are calculated by this idealized downburst model.

2) Flexibility in varying several input parameters enables this model to simulate a wide range of wind-shear intensity levels and downburst sizes.

3) Economical uses of real-time computer resources are illustrated by this model through an average execution time of 1.3 ms while occupying 383 words of memory in a Harris H800 digital computer.

## Acknowledgments

For taking part in the development of this paper, I gratefully appreciate the encouragements from John Potter and Keith Hill; I thank Julie Fulmer for typing the manuscript; and acknowledge David Babcock and Dori Wysocki for the computer calculations and preparation of the diagrams.

## References

[1]National Research Council, *Low-Altitude Wind Shear and Its Hazard to Aviation*, National Academy Press, Washington, DC, 1983, pp. 14-15.

[2]McCarthy, J. and Elmore, K., "JAWS Analysis Highlights in the Aviation Safety Context," Preprint, 29th Corporate Aviation Safety Seminar, Montreal, Canada, April 1984.

[3]Fujita, T. T., "Microbursts as an Aviation Wind Shear Hazard," AIAA Paper 81-0386, Jan. 1981.

[4]Fujita, T. T., "Tornadoes and Downbursts in the Context of Generalized Planetary Scales," *Journal of Atmospheric Sciences*, Vol. 38, Aug. 1981, pp. 1511-1534.

[5]National Center for Atmospheric Research, "The JAWS Project Preliminary Data Description," (for the Aug. 5, 1982, 1847 MDT Wind Shear Data near Stapleton International Airport, Denver, CO), National Center for Atmospheric Research, Boulder, CO, Sept. 1983.

[6]Zhu, S. and Etkin, B. E., "Fluid-Dynamic Model of a Downburst," University of Toronto, UTIAS Rept. 271, April 1983.

[7]Lamb, H., *Hydrodynamics*, 6th Ed., Dover Publications, New York, 1932, pp. 236-237.

[8]Losch, F., *Jahnke-Emde-Losch Tables of Higher Functions*, 6th Ed., McGraw-Hill Book Co. New York, 1960, pp. 43-61.

[9]Duncan, W. J., Thom, A. S., and Young, D. A., *Mechanics of Fluids*, 2nd Ed., American Elsevier Publishing Co. New York, 1970, pp. 89-94.